9-20-2022

Crop response to thermal stress without yield loss in irrigated maize and soybean in Nebraska

Sandeep Bhatti

Derek M. Heeren

Steven R. Evett

Susan A. O'Shaughnessy

Daran Rudnick

See next page for additional authors

Authors

Sandeep Bhatti, Derek M. Heeren, Steven R. Evett, Susan A. O'Shaughnessy, Daran Rudnick, Trenton E. Franz, Yufeng Ge, and Christopher M.U. Neale

Agricultural Water Management 274 (2022) 107946

Contents lists available at ScienceDirect

Agricultural Water Management

journal homepage: www.elsevier.com/locate/agwat

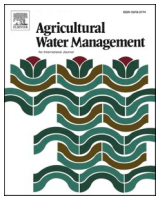

Crop response to thermal stress without yield loss in irrigated maize and soybean in Nebraska

Sandeep Bhatti [a], Derek M. Heeren [a,*], Steven R. Evett [b], Susan A. O'Shaughnessy [b], Daran R. Rudnick [a], Trenton E. Franz [c], Yufeng Ge [a], Christopher M.U. Neale [d]

[a] Department of Biological Systems Engineering, University of Nebraska-Lincoln, 3605 Fair St., Lincoln, NE 68583, USA
[b] USDA-ARS Conservation and Production Research Laboratory, 2300 Experiment Station Rd, Bushland, TX 79012, USA
[c] School of Natural Resources, University of Nebraska-Lincoln, 3310 Holdrege St., Lincoln, NE 68583, USA
[d] Daugherty Water for Food Global Institute at the University of Nebraska, 2021 Transformation Drive, Suite 3220, Lincoln, NE 68508, USA

ARTICLE INFO

Keywords:
Crop water stress$_1$
Evapotranspiration$_2$
Irrigation$_3$
Thermal sensing$_4$
Maize$_5$
Soybean$_6$

ABSTRACT

Thermal sensing provides rapid and accurate estimation of crop water stress through canopy temperature data. Canopy temperature is highly dependent on the transpiration rate of the leaves. It is usually assumed that any reduction in crop evapotranspiration (ET) leads to crop yield loss. As a result, an increase in canopy temperature due to a decrease in crop ET would indicate crop yield loss. This research evaluated the hypothesis that crop water stress could be detected using canopy temperature measurements (increased leaf temperature) from infrared thermometers (IRTs) before incurring crop yield loss. This would be possible in a narrow range when the photosynthesis rate (and carbon assimilation) is limited by solar radiation (energy-limiting water stress) while the leaf has abundant carbon dioxide for photosynthesis. Once photosynthesis becomes limited by carbon dioxide (carbon-dioxide-limiting water stress), then yield reduction would occur. In this field experiment, measured response variables included the integrated crop water stress index (iCWSI), ET, and crop yield for maize and soybean during the 2020 and 2021 growing seasons. The irrigation was applied at four different refill levels: rainfed (0%), deficit (50%), full (100%), and over (150%). The irrigation depth was prescribed using four different irrigation methods. The field was irrigated with a center pivot irrigation system, which was also used as a platform to mount IRT sensors. The iCWSI thresholds required for irrigation management were determined using the iCWSI dataset collected in 2020. The low, medium, and high iCWSI thresholds were 120, 150, and 180, respectively for maize and 110, 130, and 150, respectively for soybean. These thresholds should be updated with iCWSI data from future studies in this region to increase the credibility of the thresholds for irrigation management. The mean iCWSI values for consecutive days after a wetting event substantially increased with time for each irrigation level and a larger range in iCWSI values was observed among the irrigation levels after three days from a wetting event. The seasonal iCWSI for different levels were found to be negatively correlated with seasonal evapotranspiration for both years. The correlations between seasonal ET and crop yield were significant with the rainfed and deficit levels for maize (p-value < 0.001) and soybean (p-value $= 0.04$) in 2020. The iCWSI and yield data for the fully watered plots indicated that thermal stress was detected using the sensing system without incurring yield loss (i.e., energy-limiting water stress). The ET and yield data for 2021 indicated that reduction in seasonal crop ET did not result in yield loss which also supported the hypothesis. Future studies should investigate whether this phenomenon of detecting crop water stress in an early stage without yield loss is observed in other climates and locations.

1. Introduction

With increased pressure on freshwater resources, irrigation management focuses on maximizing crop water productivity to produce optimal yield with reduced water application. Researchers have studied the relationships between crop water stress, crop water use, irrigation, and crop yield for different cropping systems, climate, and locations (Djaman and Irmak, 2012; Eck, 1986; Hanks, 1974; Ko and Piccinni,

* Corresponding author.
E-mail address: derek.heeren@unl.edu (D.M. Heeren).

https://doi.org/10.1016/j.agwat.2022.107946
Received 8 March 2022; Received in revised form 10 September 2022; Accepted 13 September 2022
Available online 20 September 2022

2009; Musick and Dusek, 1978). These relationships inform the irrigation scheduling methods to achieve maximum productivity. Heat stress as a result of high ambient temperatures is another form of crop stress which affects crop physiology, growth, and reproduction (Lobell et al., 2015). Crop water stress information is crucial for developing various deficit irrigation strategies for improved productivity (Fereres and Soriano, 2007; Kullberg et al., 2017). Crop biomass and yield are directly affected by the incidence of crop water stress (Han et al., 2016; O'Shaughnessy et al., 2017). The plants react to crop water stress by reducing transpiration through the leaves (DeJonge et al., 2015). The timing and duration of crop water stress determines both the quantity and quality of crop yield (Aladenola and Madramootoo, 2014; Payero et al., 2006; Rossini et al., 2013; Zhang et al., 2017).

Crop yield is found to be linearly related to crop water use or ET in a majority of studies (Garrity et al., 1982; Payero et al., 2006; Schneekloth et al., 1991). The slope of this linear relationship is dependent on irrigation management, soil and residue management, climate, soil texture, hybrid characteristics, plant population, and disease pressure (Irmak, 2015). The linear relationship between crop yield and ET does not indicate direct proportional relation among the two variables. In fact, some reduction in ET may not affect crop yield if the plant has adequate concentration of carbon dioxide required for carrying out photosynthesis. Crop yield is produced as a result of photosynthesis, and crop transpiration (accounts for majority of ET following canopy closure) results from loss of water through stomata. These are two different processes which are independent of each other and are not directly affected by each other. The rate of change in photosynthesis with crop transpiration is highly dependent on the leaf-air vapor pressure difference under natural conditions (Bierhuizen and Slatyer, 1965). The water transpired by a crop and the amount of biomass accumulated during the same time are strongly connected by photosynthetically active radiation absorbed by the canopy (Monteith, 1986). We hypothesize that a crop can experience some water stress, with a reduction in transpiration causing increased leaf temperature (which can be detected for irrigation management), without a reduction in photosynthesis. The common phenomena that affect both photosynthesis and ET is stomatal conductance.

Stomatal guard cells present in crop leaves regulate the flux of water vapor lost by the leaf and the carbon dioxide entering the stomata (Medlyn et al., 2011). Stomatal conductance during the day is a function of atmospheric vapor pressure deficit and soil water content (Zhang et al., 2021b). With reduction in the stomatal conductance, the mass flux of water vapor leaving the leaf surface and the mass flux of carbon dioxide entering the leaf decreases. Hence, the changes to stomatal conductance instantly affect the crop ET through changes in the mass flow rate of water vapor. The decrease in the loss of water by transpiration results in an increase of the leaf temperature which can be detected by thermal sensors. The rate of photosynthesis is mainly driven by carbon dioxide present in the leaf and/or light energy from the sun; in a subhumid climate, in the absence of water stress, photosynthesis is often energy-limited. At the onset of water stress (reduced transpiration rate), when there is only a small decrease in stomatal conductance, the rate of photosynthesis (and production of crop biomass) may not be affected if the rate of photosynthesis is still energy-limited. With only a small reduction in stomatal conductance, the carbon dioxide concentration gradient across the stomate may increase enough to result in the same influx of carbon dioxide to the leaf, and the leaf has adequate supply of carbon to carry out photosynthesis at the optimal level along with other carbon related processes. This stage of crop water stress, in which the plant still has enough carbon for photosynthesis (i.e., energy-limited photosynthesis), will be referred to as energy-limiting water stress; we summarize this concept in Fig. 1. Carbon is sequestered by the plant at an optimal rate (similar to the rate with no crop water stress) during the energy-limiting stage of the photosynthesis. With continued reduction in the stomatal conductance below a critical level, the carbon dioxide flux rate in the leaf decreases leading to a decrease in the photosynthetic rate. This will result in a reduction in the rate of carbon assimilation (and biomass produced by the crop). This stage will be referred to as the carbon-dioxide-limiting water stress. The photosynthesis at this stage is limited by the amount of carbon present in

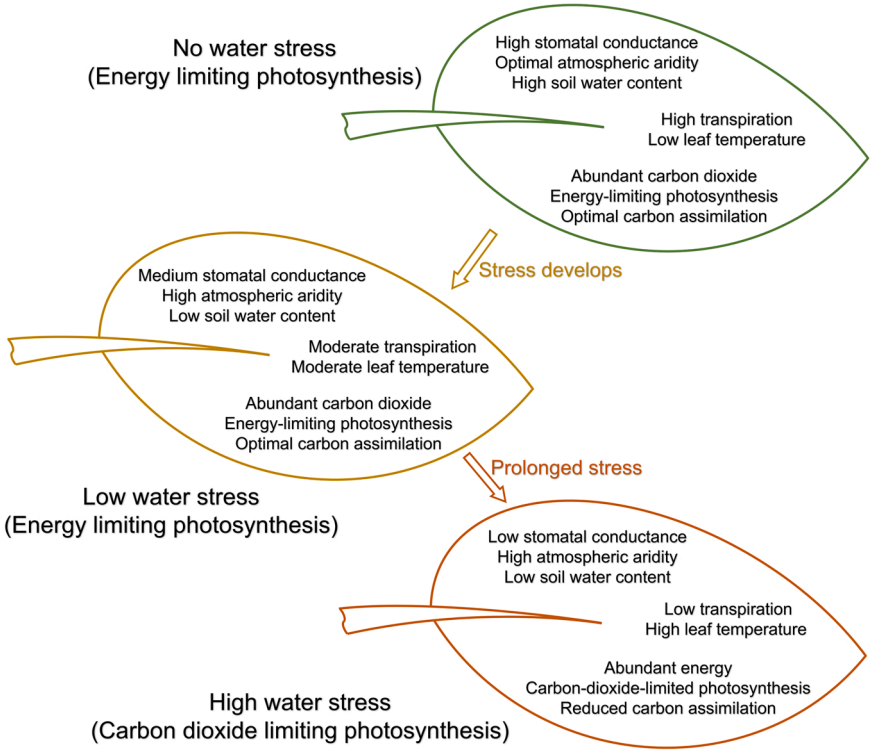

Fig. 1. Schematic of three conditions of water stress: no water stress, low water stress (energy-limiting photosynthesis), and high water stress (carbon-dioxide-limiting photosynthesis), including how the stress impacts the leaf processes.

the leaf and not by the energy available to the leaf.

Thermal sensing is widely used in research to quantify crop water stress through canopy temperature measurements (Berni et al., 2009; Kullberg et al., 2017; Lena et al., 2020; Masseroni et al., 2017; O'Shaughnessy et al., 2013; Osroosh et al., 2016; Singh et al., 2021). Canopy temperature data obtained using thermal sensing is used to determine changes to crop ET at a particular net energy (Zhang et al., 2021a). Crop water stress is commonly expressed using various thermal indices including crop water stress index (CWSI; Jackson et al., 1981), water deficit index (WDI; Moran et al., 1994), and temperature-time threshold (TTT; Upchurch et al., 1996). Canopy temperature data required to compute these indices are usually collected using IRTs installed at remote locations of the field (Payero and Irmak, 2006; Taghvaeian et al., 2012; Wanjura et al., 1995). Mounting crop canopy sensors on a center pivot irrigation system provides an opportunity to utilize the pivot lateral as a moving platform for data acquisition across the field (O'Shaughnessy et al., 2020; Stone et al., 2020; Vories et al., 2020). New center pivot systems are available with a high-speed drive, allowing the pivot lateral to make a complete revolution in a commercial-scale field (e.g., 125 ha) in only 4 h. This is significant because: 1) data can be collected without irrigating, minimizing interference from water on the canopy, yet only needing to stop irrigation for 4 h, and 2) data can be collected on the entire field at the time when detecting stress is most likely (approximately 1 h before solar noon to three hours after solar noon). A scaling algorithm (Peters and Evett, 2004) is used to estimate canopy temperature during the daylight hours for each remote location. The spatiotemporal canopy temperature data is used to compute integrated crop water stress index (iCWSI; Evett et al., 2014). The iCWSI was used as a thermal index in this study to detect crop water stress and trigger irrigation. The iCWSI integrates canopy temperature measurements throughout the day and is better at representing daily crop water stress as compared to indices using single time of day measurement of canopy temperature. The plants with high crop water stress will correspond to high iCWSI values and higher water application depth. In contrast, the plants with lower crop water stress will correspond to lower iCWSI values and requiring either no irrigation or lower application depth (O'Shaughnessy et al., 2020). The Irrigation Scheduling Supervisory Control and Data Acquisition (ISSCADA; Evett et al., 2020) system computes the spatial iCWSI maps and is capable of managing site-specific irrigation without user input. Irrigation management using thermal sensing relies primarily on leaf temperature changes that are related to transpiration rate before the onset of carbon-dioxide-limiting water stress. There is limited research on canopy thermal sensing that focuses on studying crop ET, and crop water stress before the onset of carbon-dioxide-limiting water stress. The notion of inducing crop water stress with no reduction in potential yield is not widely investigated. The detection of crop water stress in an early phase should be further explored in different locations and climates to understand the crop physiology during this phase. The moving platform for thermal sensing of crops should also be researched in the context of practical irrigation management.

This research investigated the detection of crop water stress using IRT sensors in an early phase of water stress (with energy-limited photosynthesis) without incurring crop yield loss. The iCWSI was used to determine the crop water stress. The findings from this study will also inform about the effectiveness of the irrigation scheduling methods developed on canopy temperature based thermal indices. The analyses involved evaluation of the relationships between crop yield, ET, and crop water stress for maize and soybean during the 2020 and 2021 growing seasons. The specific objectives of the study included: (1) studying the trends in iCWSI and crop yield among four different irrigation levels ranging from high stress to no stress, (2) computation of iCWSI based irrigation thresholds for maize and soybean in the sub-humid climate of eastern Nebraska, and (3) evaluating the correlations between crop yield, ET, and iCWSI for different irrigation levels.

2. Material and methods

2.1. Study site and design

A 58-ha research field situated at the University of Nebraska's Eastern Nebraska Research, Extension and Education Center (ENREEC) near Mead, Nebraska (centered at 41.172445°N, 96.478248°W) was used for this experiment during the 2020 and 2021 growing seasons. The field was divided in two halves, which were rotated between maize and soybean each year. The experiment included data from soybean in the north half in 2020, maize in the south half in 2020, maize in the north half in 2021, and soybean in the south half in 2021. The soils in the field were classified as silt loam and silty clay loam (gSSURGO, Soil Survey Staff, 2018), which were nearly equally distributed between the north and south halves. The field was irrigated using a speed-control enabled center pivot irrigation system, model Valley Irrigation 8000 (Valmont, Valley, NE), and fitted with high-speed X-Tec center drive motors.

The field area under spans six and seven of the center pivot system were used for this study. The area was divided into four radial zones and 24 arc-wise plot boundaries defining 96 plots, which were divided equally among the north and south halves (Fig. 2). The area of the plots ranged between 1870 m^2 and 2630 m^2. The four radial rings were managed using four different levels of irrigation: rainfed, deficit, full, and over. Rainfed plots were applied with no irrigation, deficit plots were applied with 50% of the full amount, full plots were applied with 100% of the prescribed irrigation, and over plots were applied with 150% of the full amount. The irrigation amount applied in the full level plots were determined using four different irrigation methods: plant feedback ISSCADA, hybrid ISSCADA, common practice, and spatial evapotranspiration model (SETMI; Neale et al., 2012).

2.2. Experimental data

Infrared thermometers (IRTs; SAPIP-IRT, Dynamax Inc., Houston, TX) were mounted on the pivot lateral and stationary posts to monitor canopy temperature. These IRTs had a field of view (FOV) of 20°. The IRTs were programmed to sense canopy temperature every five seconds and average these readings over one minute. Two IRTs were mounted for each radial zone totaling eight IRTs on the center pivot lateral. These IRTs were installed at a spacing of 6.1 m from the edges of the radial zone. The paired IRT sensors on the pivot lateral were positioned such that the FOV is pointing towards the center of the respective radial zone. A stationary IRT was installed at one full irrigated plot for each crop (Fig. 2). The stationary IRT was positioned to have a nadir view of the canopy. The height of the stationary IRT was adjusted at least once every month to maintain a constant height of 1 m above the crop canopy. More details on the position and orientation of IRTs can be found in Bhatti et al. (2022).

Soil water data from two neutron probes, model 503 Elite Hydroprobe (CPN, Concord, CA), were collected at 48 locations with a frequency of about three weeks. These 48 locations included rainfed and full irrigated plots with 24 locations in each crop. A local calibration from a nearby field (~ 3 km from the study site) with same soil types were used to calibrate the first neutron probe. The second neutron probe was cross calibrated using the first neutron probe. The slope and intercept from the calibration were 0.2738 and − 0.0991 $m^3\ m^{-3}$, respectively for the first probe, and 0.2766 and − 0.1189 $m^3\ m^{-3}$, respectively for the second probe. The data were acquired at depths of 15, 45, 76, and 107 cm. The soil water content representing 122 cm deep root zone was computed using depth weighted average of neutron probe readings from the four depths. Soil water data was also monitored using Acclima soil water sensors (Acclima, Inc., Meridian, ID) at one location for each crop. These sensors were installed horizontally at depths of 15, 30, 46, and 76 cm for each location.

Weather data for the ISSCADA system including air temperature, wind speed, wind direction, rainfall, relative humidity, and solar

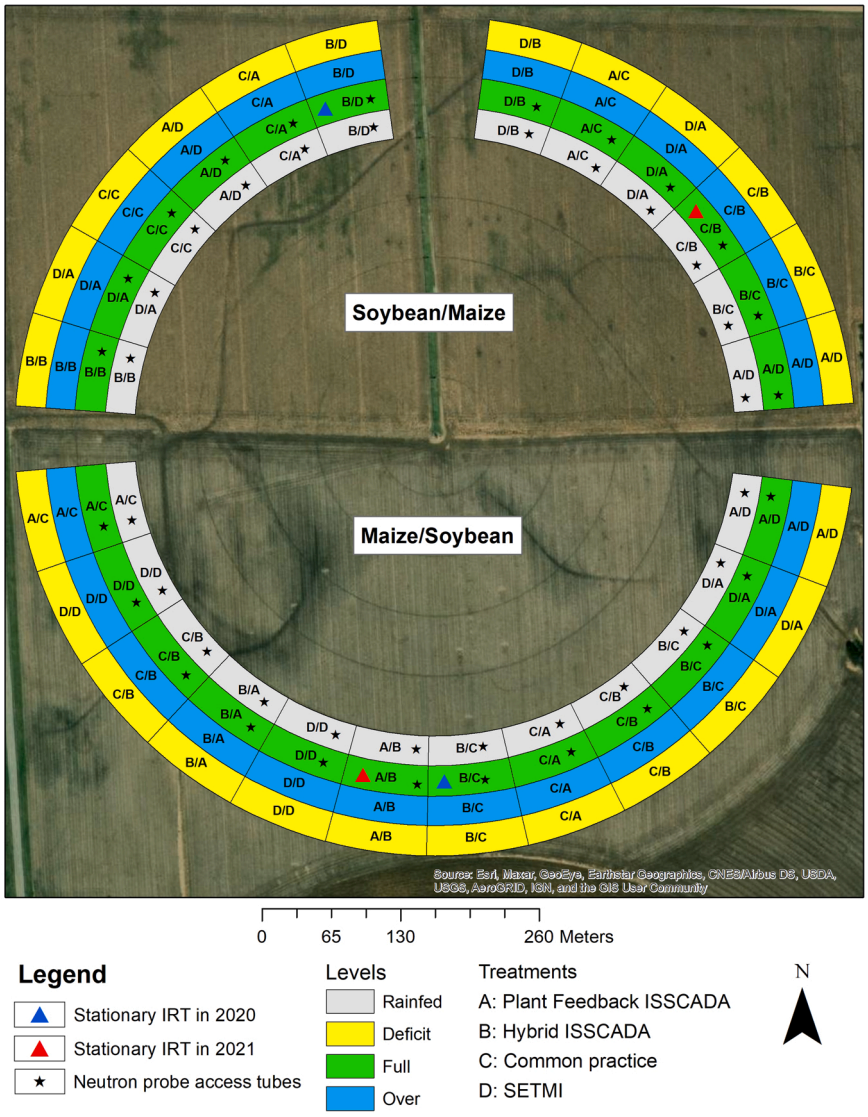

Fig. 2. Layout of experimental plots used in the study during 2020 and 2021 growing seasons. Letters used in the plot denote irrigation methods applied in 2020/2021. World imagery from ESRI ArcMap was used as the background basemap.

radiation, were obtained using an AgSense weather station (Valmont Industries Inc., Huron, SD). These weather variables were recorded at a frequency of 5 min. The weather station was installed just west of the field in an open area with grass. The cup anemometer was installed at a height of 3 m. For the SETMI model, weather data from Memphis 5 N station (Nebraska Mesonet) were used at hourly and daily time step. This station was about 5 km away from the field.

Remote sensing imagery from PlanetScope (Planet Labs, Inc., San Francisco, CA) was used in SETMI. The resolution of the imagery was 3 m and was acquired at a daily time step. Images were inspected for cloud cover using ArcMap 10.4.1 (ESRI, Redlands, CA), and images having cloud cover over or around the field were not included in the model. The red and near infrared bands of the imagery were used in the model to compute the soil adjusted vegetation index (SAVI; Huete, 1988).

2.3. Irrigation management

The irrigation was managed using four irrigation scheduling methods applied at four different irrigation levels. The ISSCADA system was used to prescribe two methods: plant feedback and hybrid. The plant feedback method used IRTs on the center pivot and the stationary posts along with weather data to compute spatial iCWSI maps. The iCWSI data were used to schedule irrigation for the plant feedback method. In addition to iCWSI data, the hybrid method also used soil water data acquired from Acclima soil water sensors. The third method was the common practice, which included soil sampling using a soil probe and using the hand feel method on the sampled soil to make an irrigation recommendation. The fourth method was scheduled using the SETMI model, which used PlanetScope imagery and soil water data from neutron probe. The SETMI model was used for irrigation recommendations similar to Bhatti et al. (2020). This model computed spatial soil water balance at 3 m pixel resolution and recommended irrigation at a sub-field scale (experimental plots). The irrigation recommendations obtained from these four methods were applied at four levels: 0% or rainfed, 50% or deficit, 100% or full, and 150% or over. This study focused on the differences in response variables found among different levels of irrigation. The evaporation loss during irrigation applications was expected to be larger in the deficit level since the irrigation depth was smaller in deficit as compared to the other irrigated levels. There were 10–11 irrigation events applied in 2020 and 4–5 irrigation events applied in 2021 for both crops. The mean seasonal irrigation depth prescribed for the four levels are given in Table 1.

Table 1
Mean seasonal irrigation depth prescribed for four different levels in 2020 and 2021.

Level	Maize 2020	Soybean 2020	Maize 2021	Soybean 2021
Rainfed	0	0	0	0
Deficit	118	94	46	28
Full	236	188	92	56
Over	354	282	138	84

2.4. Computation of response variables

2.4.1. Integrated crop water stress index

The crop water stress was represented using iCWSI computed by the ISSCADA system. The iCWSI is more descriptive of the cumulative crop water stress during a day as compared to other thermal indices utilizing only single measurement of canopy temperature. The thermal data from the IRT sensors on the stationary post and pivot lateral were used to compute the iCWSI. The center pivot was moved to complete a revolution without running water (dry scan) during the daylight hours for data collection from the pivot-mounted IRTs. In total, there were 16 dry scans conducted in 2020, and 19 dry scans conducted in 2021 (Table 2). A temperature scaling algorithm (Peters and Evett, 2004) was used to estimate canopy temperature for each remote location on a diurnal basis. The algorithm also used data from the stationary IRTs installed at the full level plots in both crops. The iCWSI was computed by integrating the crop water stress index (CWSI; Jackson et al., 1981) over peak daylight hours (9:00 AM to 7:00 PM) at a time step of 1 min. The iCWSI at a given location was computed as mentioned in O'Shaughnessy et al. (2017) (Eq. 1):

$$iCWSI = \sum_{i=1}^{N} \frac{(T_c' - T_a) - (T_c - T_a)_{ll}}{(T_c - T_a)_{ul} - (T_c - T_a)_{ll}} \quad (1)$$

where i is the ith time step, N is total number of one-minute steps between 9:00 AM and 7:00 PM, T_c' is canopy temperature estimated using scaling algorithm, T_a is ambient air temperature, $(T_c - T_a)_{ll}$ represents the lower limit of the canopy and air temperature differential, and $(T_c - T_a)_{ul}$ represents the upper limit of the canopy and air temperature differential. The lower and upper limits of the temperature difference between canopy and air were computed using the theoretical CWSI approach (Jackson et al., 1981).

The iCWSI computed for each location was used to produce spatial crop water stress maps for the field on a given day. The GPS data from the pivot were used to georeference the iCWSI data. The ISSCADA system outputs the iCWSI maps at a resolution of 2°. The iCWSI values for locations lying within a radial zone were averaged to compute a representative value of iCWSI for that zone.

Table 2
Days when the pivot was moved dry to collect data from pivot-mounted sensors in 2020 and 2021. The cloud cover increases in the order of clear, scattered, partly cloudy, mostly cloudy, and overcast. The cloud cover was determined using the solar radiation data collected by the AgSense weather station. The times are mentioned in Central Time zone.

Date *2020*	Time of scan	Cloud cover	Date *2021*	Time of scan	Cloud cover
Jul 21	12:25–16:34	Partly cloudy	May 23	11:25–15:30	Mostly cloudy
Aug 04	12:26–16:31	Mostly cloudy	Jun 04	10:33–14:40	Scattered
Aug 09	10:36–14:43	Scattered	Jun 05	13:09–17:15	Partly Cloudy
Aug 10	13:13–17:20	Scattered	Jul 02	11:06–15:14	Partly Cloudy
Aug 11	13:02–17:08	Partly cloudy	Jul 06	11:28–15:31	Scattered
Aug 12	10:06–14:12	Mostly cloudy	Jul 08	10:33–14:40	Mostly cloudy
Aug 17	09:56–15:22	Clear	Jul 20	11:30–15:36	Scattered
Aug 18	09:50–15:16	Mostly cloudy	Jul 26	11:30–15:37	Clear
Aug 19	11:58–17:23	Partly cloudy	Jul 30	11:47–15:55	Mostly cloudy
Aug 20	12:16–16:23	Mostly cloudy	Aug 02	12:13–16:22	Partly cloudy
Aug 26	10:29–14:35	Clear	Aug 04	11:43–15:52	Scattered
Aug 27	13:16–17:22	Clear	Aug 16	12:31–16:40	Clear
Sep 08	10:01–14:07	Overcast	Aug 18	14:02–18:15	Partly cloudy
Sep 14	10:24–15:50	Clear	Aug 23	11:32–15:43	Partly cloudy
Sep 15	10:30–15:56	Scattered	Aug 24	12:56–17:06	Clear
Sep 16	11:10–16:37	Partly cloudy	Sep 08	11:25–15:33	Clear
			Sep 10	11:22–15:39	Scattered
			Sep 11	11:30–15:40	Partly cloudy
			Sep 15	11:20–15:28	Clear

2.4.2. SETMI modeled evapotranspiration

SETMI was used to model spatial ET using PlanetScope satellite imagery. The dual crop coefficient approach was used to compute crop ET (Allen et al., 1998). The model computed SAVI values were used to compute reflectance based-crop coefficients (Campos et al., 2017). The alfalfa-based reference ET was computed using the ASCE Standardized Tall Reference Evapotranspiration equation (ASCE-EWRI, 2005). The reference ET was computed at hourly time step and added up to daily time step. The weather data for reference ET was acquired from the Memphis 5 N station (Nebraska Mesonet). The SETMI modeled ET was computed for all four irrigation level plots. The field capacity for the plots were estimated using the first neutron probe soil water measurement taken on June 12, 2020 (observational field capacity). The field received rainfall of about 10 mm two days prior to the measurement day. The model was not updated with soil water data when computing modeled ET since there were no soil water data for the deficit and over plots.

2.4.3. Measured evapotranspiration

Soil water balance adjusted with neutron probe measurements in SETMI was also used to compute seasonal crop ET. These ET values computed from soil water balance were referred to as measured ET since soil water data were used to update the water balance. SETMI was used to output seasonal deep percolation and runoff. The soil water storage term on a seasonal basis was computed from the difference between first and last neutron probe measurements. The neutron probe data was used to represent a root zone depth of 122 cm. During the 2020 season, it was possible that the rainfed crop may have extracted some water from depths greater than 122 cm which were not accounted for in the measured ET. The measurement period (first and last neutron probe measurement day) used to represent seasonal ET for each crop is shown in Table 3. This measurement period was used for representing the seasonal ET for each crop-year. The measured ET was only computed for

Table 3
Planting date, harvesting date and neutron probe measurement period for the different crop-year combinations. The seasonal evapotranspiration was computed for this measurement period.

Crop	Planting date	Harvesting date	Measurement period
Maize 2020	April 24	Oct 13	June 12 - Sept 25
Soybean 2020	May 2	Sept 28	June 12 - Sept 25
Maize 2021	April 28	Oct 8	June 4 - Sept 24
Soybean 2021	May 13	Oct 21	June 8 - Sept 24

the rainfed and full level plots since soil water data was only measured in these plots.

2.4.4. Crop yield

The crop yield data were recorded using yield monitoring equipment (model John Deere 2630 Yield Monitor System with RTK GPS accuracy) on the combine harvesters (model John Deere S650). The combine yield monitors were calibrated at the beginning of each season following Original Equipment Manufacturer procedure. The yield monitors have an expected accuracy range of ± 3% and were recalibrated if the error was higher than the expected range. Similar yield monitoring equipment were utilized in Barker et al. (2018); Bhatti et al. (2020). The yield data were processed and filtered using the Yield Editor software version 2.0 (Agricultural Research Service, United States Department of Agriculture). The processed yield was compared to the weighing grain cart readings to validate the processed data. The grain moisture was removed to compute dry grain during yield processing and the dry yield was used to conduct the analysis. The plot yield for each crop was computed by averaging the yield points within the plot using ArcGIS 10.4 software (ESRI, Redlands, CA).

2.5. Data analysis

The response variables used for analyses included crop yield, iCWSI, and crop ET. These variables were correlated to study the type and strength of correlation. An inner buffer of 6.1 m around the edges of each plot was used to remove boundary effects from adjacent plots. The data collected from the buffer area of each plot were excluded from the analyses. The iCWSI data collected between August 4 and 20 were used for maize and soybean in 2020. For 2021, the iCWSI data used for maize were collected between July 2 and August 24, and for soybean were collected between July 20 and August 24. The soil had significant interference in the iCWSI data for soybean before July 20, 2021, since the canopy was not completely covering the soil. These measurement periods for iCWSI represented fully grown crop with canopy closure before the onset of crop senescence. The iCWSI data for different analyses were compared among the four irrigation refill levels.

The iCWSI data collected from the dry scans were averaged under different scenarios. These scenarios included combined (all data), sunny days, cloudy days, more than two days from a wetting event, more than three days from a wetting event, and within 2 days of a wetting event. The classification of cloud cover on a certain day was determined using the incoming solar radiation data collected by the AgSense weather station. The radiation data were investigated for the periods during a day when there was a significant decrease in solar radiation from its upper limit. The day was classified as cloudy if the incoming solar radiation was lower than the upper potential limit for more than 25% of the time during the daylight hours. Further, the iCWSI data collected in 2020 were used to define thresholds for irrigation scheduling in 2021. A total of three thresholds were computed to indicate low, medium, and high stress. The iCWSI data collected between August 4 and August 20 were used to compute these thresholds. There were total of nine dry scans conducted between these days. The iCWSI data collected only from the full irrigated plots were used for the computation of these thresholds. The high threshold was computed by averaging the iCWSI data collected after two or more days from a wetting event (rainfall or irrigation). The low threshold was computed by averaging the iCWSI data acquired within two days of a wetting event. The average value of the high and low thresholds was used for computing the medium threshold.

The relation between iCWSI and wetting events was investigated using data acquired on consecutive days after a wetting event. There were two instances in 2020 where iCWSI data were collected successively for four days after a wetting event. However, there was only one instance in 2021 where iCWSI data were collected during 7–13 days after a wetting event. The iCWSI data for this analysis were averaged for each irrigation level plots and differences in iCWSI values among the different levels were also discussed.

The seasonal crop ET was computed for the respective neutron probe measurement period for each case (Table 3). The daily values of ET were added for all days within the measurement period to compute the seasonal ET. The modeled ET computed from SETMI, and the measured ET computed from water balance were compared on a seasonal basis. Since the neutron probe data was not available for the deficit and over levels, the SETMI model was not updated with neutron probe data during the modeling of seasonal ET. The coefficient of determination (r^2) along with the regression equation were determined. This comparison was made using rainfed and full irrigated plots.

The iCWSI and ET data were correlated for both crops in 2020 and 2021. The iCWSI data acquired after two or more days from a wetting event were used for this analysis (Table 5). The data for each irrigation level were then averaged over the selected dry scan days to get a single average iCWSI value for each level. There were total of 12 plots that were used to average iCWSI data for each irrigation level in each crop. The seasonal ET was also averaged among the plots for each level. The measurement period mentioned in Table 3 was used for computing the seasonal ET. The plot averaged seasonal measured ET and iCWSI were correlated for the rainfed and full level plots. The seasonal modeled ET and iCWSI correlation was investigated for all four levels.

The crop yield and seasonal ET were also correlated at plot scale for both years. The correlation used with measured ET was conducted for rainfed and fully irrigated plots. The correlation used with modeled ET was conducted for all four levels. For the modeled ET analysis, two regressions were computed: the first regression between the rainfed and deficit plots, and the second regression between the full and over level plots. It was investigated whether the first regression yielded a positive slope, and the second regression had a zero slope. Statistical t-tests were conducted at a 5% significance level to investigate if the slope of the correlations were different from zero.

The r^2, linear regression analysis, root mean square error (RMSE), and statistical tests were conducted using the Microsoft Excel (Microsoft Corporation, Redmond, WA). The least squares method was used to select the linear regression model. The RMSE was computed using the following equation:

$$\mathrm{RMSE} = \sqrt{\frac{1}{n}\sum_{i=1}^{n}(S_i - O_i)^2} \quad (2)$$

where S_i are predicted values, O_i are observations, and n are number of observations.

3. Results and discussion

3.1. Mean weather conditions

The weather variables presented for both study years were computed between June 1 and September 30 (Table 4). The average daily maximum and minimum temperature were similar for 2020 and 2021. The total rainfall depth in 2020 was smaller than half of the total rainfall depth received in 2021. A weather station (Mead 6 S, National Centers

Table 4
Average weather conditions between June and September for 2020 and 2021. The hourly weather data was acquired from Nebraska Mesonet's weather station. The wind speed was monitored at a height of 3 m.

Parameters	2020	2021
Max temperature (°C)	28.9	29.2
Min temperature (°C)	16.6	16.1
Wind speed (m s^{-1})	3.5	3.2
Relative humidity (%)	58	58
Vapor pressure deficit (kPa)	1.6	1.6
Incoming solar radiation (W m^{-2})	549	541
Rainfall (mm)	178	386

for Environmental Information) close to the field (~6.5 km) reported a historic average rainfall (1991–2020) of 381 mm between the months of June and September. Hence, the 2020 growing season was extremely dry for this region. The average wind speed, relative humidity, vapor pressure deficit, and solar radiation were computed for daylight hours from 9 AM to 7 PM.

3.2. Seasonal water inputs and crop water stress

The seasonal iCWSI, rainfall, and irrigation data for the four crop-year scenarios in common practice plots were shown using Fig. 3. The rainfall events among the two seasons were observed to be different primarily in terms of rainfall depth. The rainfall in the second half of the 2021 growing season experienced substantially larger rainfall events as compared with 2020. There were seven rainfall events larger than 25 mm in 2021 as compared to only one in 2020. The seasonal irrigation depth applied in 2020 was larger as compared with 2021 (Table 1). The iCWSI data for 2020 had higher values on average as compared to 2021. The iCWSI data from mid-May to mid-June in 2021 indicated high crop water stress because of small canopy cover and significant soil interference in the background for both crops. Crop water stress was also high in 2020 towards the end of the season, which could be attributed to the effects of senescence on crop physiology.

The iCWSI data were averaged for the sunny days, cloudy days, all measurement days, or certain number of days from a wetting event to study how these conditions affect the crop water stress. The averaged iCWSI values for all four crop-years are listed in Table 5. In 2020, the average iCWSI values ranged between 118 observed in over and 254 observed in rainfed for maize. The soybean iCWSI values ranged between 109 observed in over and 201 observed in rainfed. The iCWSI among the irrigation levels increased in the order of over, full, deficit, and rainfed for both crops. This observation was consistent with Kashyap (2021) in which high-frequency unmanned aircraft flights were conducted to acquire thermal imagery of soybean at this field site on August 26, 2020. He found that the difference in canopy and air

Table 5
Averaged iCWSI values under different scenarios for the different levels in 2020 and 2021. The irrigation levels included rainfed (0%), deficit (50%), full (100%), and over (150%). The different scenarios included data from all dry scan days, sunny days, cloudy days, more than two days from a wetting event, more than three days from a wetting event, and within two days of a wetting event.

Scenario	Rainfed	Deficit	Full	Over
Maize 2020				
Combined	178	157	144	138
Sunny	165	147	137	132
Cloudy	193	169	152	145
More than 2 days from wetting event	224	195	175	168
More than 3 days from wetting event	254	221	196	190
Within 2 days of wetting event	145	130	122	118
Soybean 2020				
Combined	157	125	119	114
Sunny	152	124	120	117
Cloudy	170	134	126	118
More than 2 days from wetting event	201	153	142	135
More than 3 days from wetting event	196	170	159	151
Within 2 days of wetting event	132	113	111	109
Maize 2021				
Combined	84	82	77	84
Sunny	81	78	73	81
Cloudy	104	102	94	102
More than 2 days from wetting event	98	95	89	97
More than 3 days from wetting event	125	124	117	130
Within 2 days of wetting event	55	52	48	56
Soybean 2021				
Combined	70	67	64	70
Sunny	73	69	66	72
Cloudy	86	81	77	83
More than 2 days from wetting event	98	95	89	97
More than 3 days from wetting event	100	95	91	97
Within 2 days of wetting event	34	31	30	35

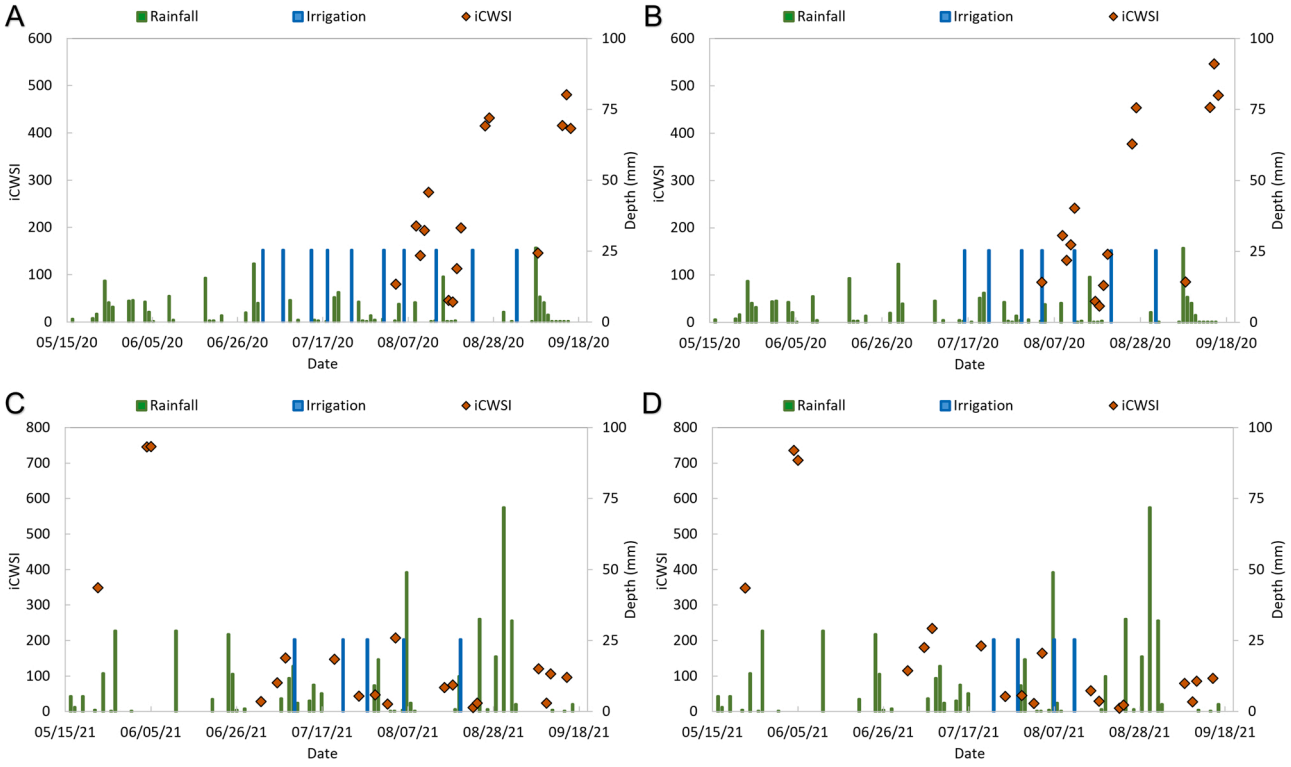

Fig. 3. Time series data of rainfall, irrigation, and iCWSI for A) maize 2020, B) soybean 2020, C) maize 2021, and D) soybean 2021. The iCWSI data was plotted using the left y-axis, and water depths were plotted using the right y-axis.

temperature followed a clear diurnal pattern, and the canopy temperature for the full level was consistently higher than the canopy temperature for the over level throughout the day. In 2021, the average iCWSI values ranged between 48 observed in full and 130 observed in over for maize. The iCWSI values ranged between 30 observed in full and 100 observed in rainfed for soybean. It is evident that average iCWSI values in 2020 were nearly double than that observed in 2021 for both crops. The reason for higher crop water stress in 2020 could be attributed to smaller rainfall depth and larger available energy (i.e., higher average solar radiation) than 2021 (Table 4). Further, it was observed that the over level experienced similar crop water stress as rainfed crop in 2021 as indicated by average iCWSI data shown in Table 5. The high crop water stress observed in over could be due to anaerobic conditions and low oxygen in the root zone as a result of over application of water (Pezeshki, 2001; Wu et al., 2018). The iCWSI values observed for sunny days were consistently lower than for the cloudy days. This observation could be attributed to more diffused radiation available on cloudy days than on sunny days (Durand et al., 2021).

The average iCWSI values for full irrigated plots were used for defining the low, medium, and high iCWSI thresholds. Since the full irrigated plots were managed to experience crop water stress without incurring yield loss, the thresholds were computed only using these plots. The data from the full irrigated plots on a given dry scan day were averaged to compute a single averaged value of iCWSI. The iCWSI values obtained by averaging data collected after two or more days from a wetting event were 180 for maize and 150 for soybean, which were used as the high threshold. The iCWSI values obtained by averaging data collected within two days of a wetting event were 120 for maize and 110 for soybean, which were used as the low threshold. The mean of the respective low and high thresholds was used for the medium threshold for both crops. In summary, the low, medium, and high thresholds for maize were 120, 150, and 180, respectively and for soybean were 110, 130, and 150, respectively. These values corresponded to different irrigation depths prescribed by the ISSCADA system: 12.7 mm for the low threshold, 19 mm for the medium threshold, and 25.4 mm for the high threshold. Crop exposure to water stress during the early vegetative stages will reduce the vegetative cover and during the reproductive stages will impact the grain yield. Prolonged iCWSI readings above the low threshold for several days will likely result in crop yield loss from the potential crop yield for the season. The high iCWSI threshold denotes higher crop water stress as compared to low or medium threshold and indicates immediate need to irrigate the crop to avoid crop yield loss.

It is expected that these iCWSI thresholds used for ISSCADA system should be transferrable to locations with similar climate in the Central Great Plains. These iCWSI thresholds were used for managing irrigation for the ISSCADA methods in 2021. The crop yield observed in the ISSCADA plots were not significantly different from other irrigation methods in 2021. Since 2021 was significantly wetter than 2020, these thresholds should be further tested for irrigation management of maize and soybean to evaluate the suitability of these thresholds over multiple seasons with varying weather conditions. The 2021 iCWSI data were not used for computing the final thresholds since significant crop water stress was not observed during this season and there were small differences in crop water stress between the irrigation levels. It is recommended to incorporate iCWSI data from two more seasons in the computed thresholds. These iCWSI thresholds could still be used for implementation of the ISSCADA system in this region and could be further updated with data from additional seasons.

3.3. Crop water stress after a wetting event

In 2020, iCWSI data from two intervals were used for investigating

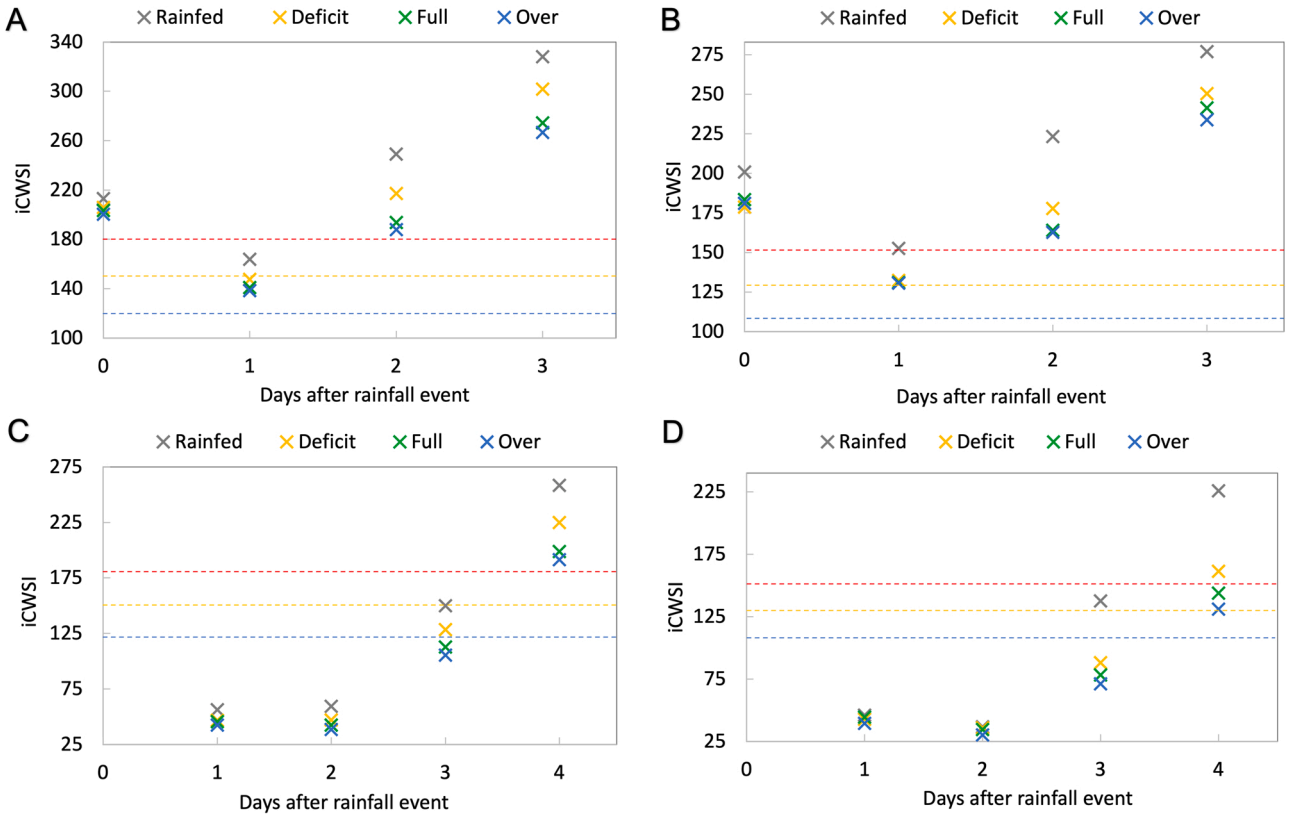

Fig. 4. Average iCWSI values for each irrigation level plotted against days after a wetting event in 2020: A) maize after 8 mm rainfall on August 9, B) soybean after 8 mm rainfall on August 9, C) maize after 18 mm rainfall on August 16, and D) soybean after 18 mm rainfall on August 16. The dashed blue, yellow, and red lines in the plots denotes the low, medium, and high iCWSI thresholds developed for maize and soybean. (For interpretation of the references to colour in this figure legend, the reader is referred to the web version of this article.)

the trend between iCWSI and wetting events. The two intervals included iCWSI data from August 9–12 (Fig. 4A and B) and August 17–20 (Figs. 4C and 4D). The wetting events before these two intervals were 8 mm rainfall on August 9 and 18 mm rainfall on August 16. The rainfall event on August 9 occurred between 5:30 and 8:30 AM, which was before the data collection from the pivot-mounted sensors on that day. It was observed that the iCWSI increased for all levels with each day after the wetting events for both crops (Fig. 4). An exception to this observation was found for data on August 9 and 10, where iCWSI values decreased on the next measurement day. The rainfall event on August 9 had occurred just two hours before the dry scan was conducted. The decrease in iCWSI on August 10 may be attributed to the delay in response of the crop canopy to the added water in the soil root zone through the rainfall event. The variability in iCWSI among the four levels also increased with each day after the wetting events. For the data between August 17 and 20, the range of average iCWSI among the four levels increased from 14 during day 1–67 during day 4 after the wetting event for maize, and from 6 during day 1–95 during day 4 after the wetting event for soybean. The rainfed crop had the largest iCWSI values among the four levels for each measurement day. The average dry maize yield observed for the rainfed, deficit, full, and over levels were 11.8, 13.1, 13.6, and 13.7 Mg ha^{-1}, respectively. The average dry soybean yield observed for rainfed, deficit, full, and over levels were 4, 4.4, 4.4, and 4.5 Mg ha^{-1}, respectively. The rainfed maize and rainfed soybean had significantly lower yield than the respective irrigated crops. Therefore, the iCWSI values obtained for the rainfed crop indicated carbon-dioxide-limiting water stress. However, the iCWSI values obtained for the full and over levels indicated the energy-limiting water stress. These results show that the crop water stress could be detected before the onset of carbon-dioxide-limiting water stress and could be used for real time irrigation scheduling.

In 2021, the iCWSI data was not available immediately following a wetting event. The iCWSI data collected between July 2 and 8 following a rainfall event of 38 mm on June 25 was presented for both crops. Similar to 2020, the iCWSI values for all levels increased from 7 day to 13 days after the wetting event (Fig. 5). The soybean iCWSI values were much larger than maize iCWSI for this case. This was due to the low canopy cover in soybean (~ 60% canopy cover) and significant interference from the soil surface. The range in iCWSI values among the four levels increased from 3 to 12 for maize and 5–24 for soybean. The average dry maize yield observed for the rainfed, deficit, full, and over levels were 14.6, 14.8, 15.0, and 14.8 Mg ha^{-1}, respectively. The average dry soybean yield observed for rainfed, deficit, full, and over levels were 5.0, 4.9, 4.9, and 5.0 Mg ha^{-1}, respectively. The maize and soybean yield obtained in 2021 were not significantly different among the different irrigation levels. Since the yields were similar among the four levels, it can be implied that the iCWSI values computed for the four levels predominantly detected the energy-limiting water stress in 2021. In summary, the iCWSI data indicated considerable differences among the irrigation levels, but there were no differences observed in crop yield among the levels. Therefore, the iCWSI data could be effectively used to detect stress signals for scheduling irrigation without incurring any yield loss.

3.4. Modeled and measured evapotranspiration

The seasonal modeled and measured ET were compared for all four crop-year cases (Fig. 6). The plots from the rainfed and full levels were used for this comparison since the soil water data was only available from these plots. The range of measured ET among the different plots for maize were 299 mm as compared to 217 mm estimated by modeled ET in 2020. The range of soybean ET was also larger for measured ET (183 mm) as compared with modeled ET (151 mm). It was found that the linear correlations between the measured and modeled ET were strong for both crops in 2020. The r^2 observed for these correlations was 0.90 and 0.88 for maize and soybean, respectively. The RMSE obtained for maize was 38 mm and for soybean was 32 mm. The linear correlations were close to the 1:1 line (Fig. 6). The modeled ET were able to capture about 88% of the variability observed in measured ET. The range of measured ET among the plots for maize was 299 mm and for soybean was 183 mm in 2020. In contrast, the range of modeled ET was about 217 mm and 151 mm for maize and soybean, respectively. The larger range observed in measured ET was primarily due to variability in the soil water storage term of the water balance computed using neutron probe data. The neutron probe data was used to represent the root zone to a depth of 122 cm. Since 2020 was a dry year, it is possible that rainfed crop had used soil water from depths larger than 122 cm and may have induced some uncertainty in measured ET for rainfed plots. The two-source energy balance approach of the SETMI model was not implemented for modeling ET due to logistical time constraints and unavailability of thermal imagery. This approach could also capture the variability in the crop ET among the different plots.

In 2021, the range of modeled ET (91 mm for maize and 77 mm for soybean) was comparable to that observed for measured ET (109 mm for maize and 92 mm for soybean) for both crops. The linear correlations were not as strong as was observed in 2020. The r^2 observed for both crops in 2021 was between 0.42 and 0.49. The RMSE obtained for maize and soybean was 75 and 52 mm, respectively. The weaker correlation in 2021 as compared with 2020 could be attributed to differences in surface runoff between the two years. The runoff estimated by the model

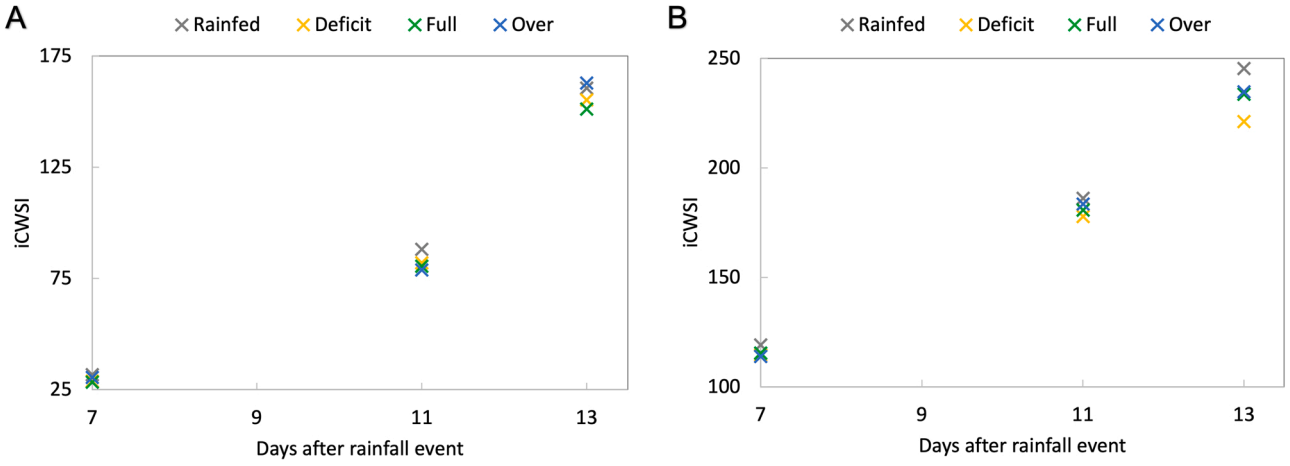

Fig. 5. Average iCWSI values for each irrigation level plotted against days after a wetting event in 2021: A) maize after 38 mm rainfall on June 25, and B) soybean after 38 mm rainfall on June 25.

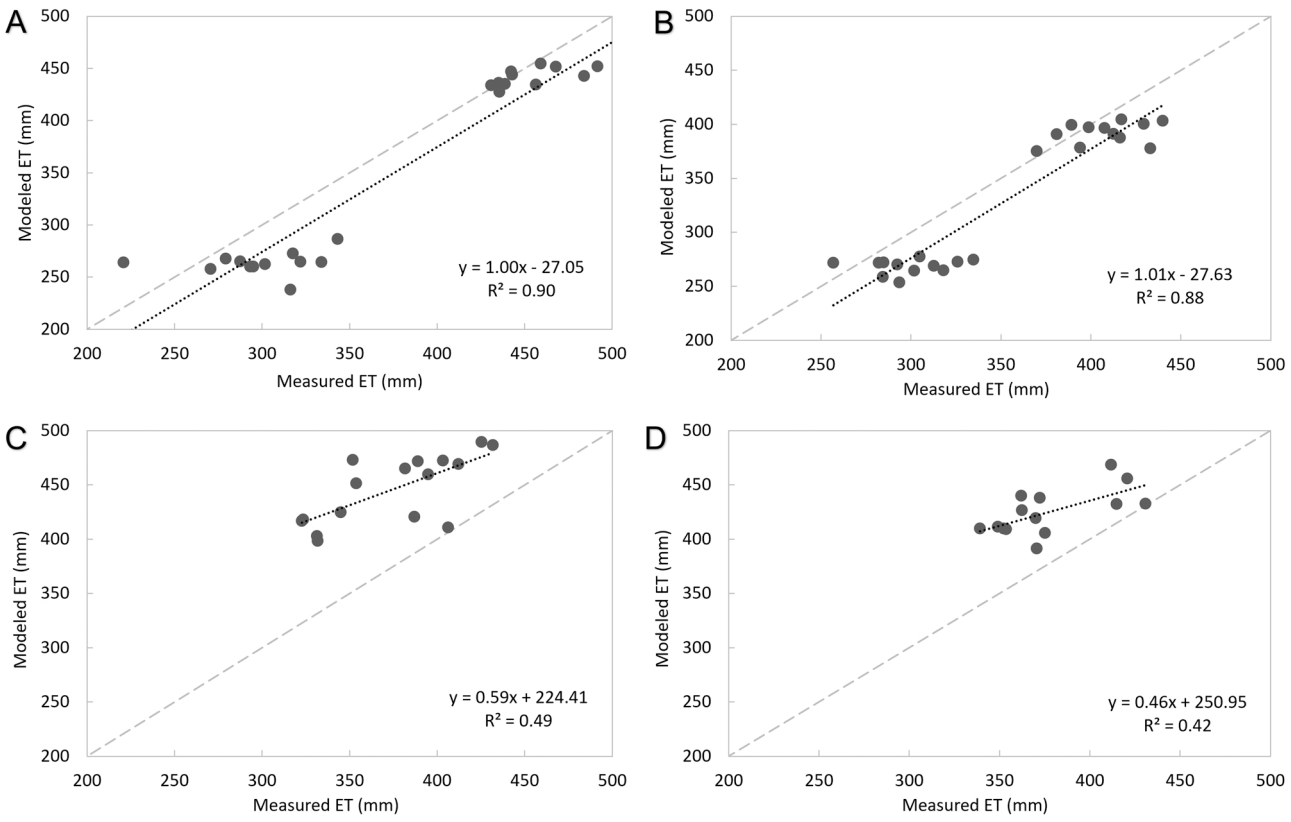

Fig. 6. Relation between measured and modeled evapotranspiration using data from rainfed and full irrigation level plots for both crops in 2020 and 2021: A) maize 2020, B) soybean 2020, C) maize 2021, and D) soybean 2021. The dashed light grey line in the figure is a 1:1 line. The SETMI model was used to compute the modeled ET and seasonal water balance was used to compute the measured ET.

was 3 mm in 2020 and 58 mm in 2021. Further, the measured ET was directly affected by the computed runoff value as measured ET was estimated from the water balance equation. However, the modeled ET was primarily computed from the dual crop coefficient approach and may not account for runoff explicitly. Further, the root zone depletion adjustment using the mean difference method and neutron probe data (Bhatti et al., 2020) was tested to improve modeled ET results. However, the adjusted modeled ET had high RMSE and lower r^2 when compared to the model results without the adjustment and was not used for analysis. It was concluded that neutron probe data for all plots was required as an input to the model for improved results. In conclusion, the variability in crop ET captured by the measured ET was larger as compared to the modeled ET for all four crop-year combinations. There were larger differences in crop ET observed among rainfed and irrigated crops using both measured and modeled methods in 2020 as compared to 2021. The 2020 season had less rainfall, which caused the rainfed plots to have substantially lower crop ET in 2020.

3.5. Crop water stress, evapotranspiration, and crop yield

The average iCWSI was correlated with seasonal ET for the different irrigation levels. The seasonal ET was modeled for all four levels. However, the measured ET obtained from the water balance could only be computed for the rainfed and full levels. The mean iCWSI in 2020 ranged from 168 in over to 225 in rainfed for maize, and 135 in over to 201 in rainfed for soybean. The iCWSI range was smaller for both crops in 2021 (between 77 and 98). The crop water stress is known to increase with a decrease in stomatal conductance and crop ET (DeJonge et al., 2015; Zhang et al., 2021b). This relation was found to be consistent for both crops during both growing seasons. Negative linear correlations were observed among all levels for maize and soybean in both years (Fig. 7). The mean iCWSI for rainfed was significantly higher from the other irrigated levels in 2020 since the confidence interval of iCWSI for rainfed was larger than that of the other levels. The standard error in iCWSI ranged between 8 and 10 for 2020 and between 6 and 8 for 2021. An anomaly to this relationship was found in the over level in 2021. The over irrigation level had the largest seasonal crop ET among the levels, but the mean iCWSI was found to be larger than deficit and full levels for both crops. The over application in the over level plots could have negatively impacted the crop due to waterlogging issues and/or leaching of nutrients. In 2020, the mean iCWSI was larger for deficit as compared to full for both crops even with no significant differences in yield and noticeable differences in crop ET (55 mm for maize and 26 mm for soybean on average). In 2021, the mean iCWSI data were different among the irrigation levels indicating that the IRTs were able to sense differences among the treatments even when there were no yield differences observed for both crops.

Crop yield was correlated with seasonal ET modeled using SETMI for maize and soybean (Fig. 7). The data points computed using the average crop yield and seasonal ET for each refill level were also shown in the figure for each crop-year. The data points for rainfed and deficit were used to compute one regression and the data points for full and over were used to compute the second regression. It was investigated if the first regression had a positive slope between rainfed and deficit, and the second regression had a zero slope between full and over. A positive slope indicated an increase in yield with an increase in ET. A zero slope will indicate no increase in yield with an increase in ET. There were significant positive correlations observed between rainfed and deficit for both maize (p-value < 0.001) and soybean (p-value $= 0.04$) in 2020. In all other cases, the slopes of correlations were no different than zero (p-value > 0.05). The correlations observed in 2021 were found to be no different than zero for both crops depicting that reduction in seasonal ET for the different irrigation levels did not result in a yield loss.

It can be observed from Fig. 8 that there was more separation

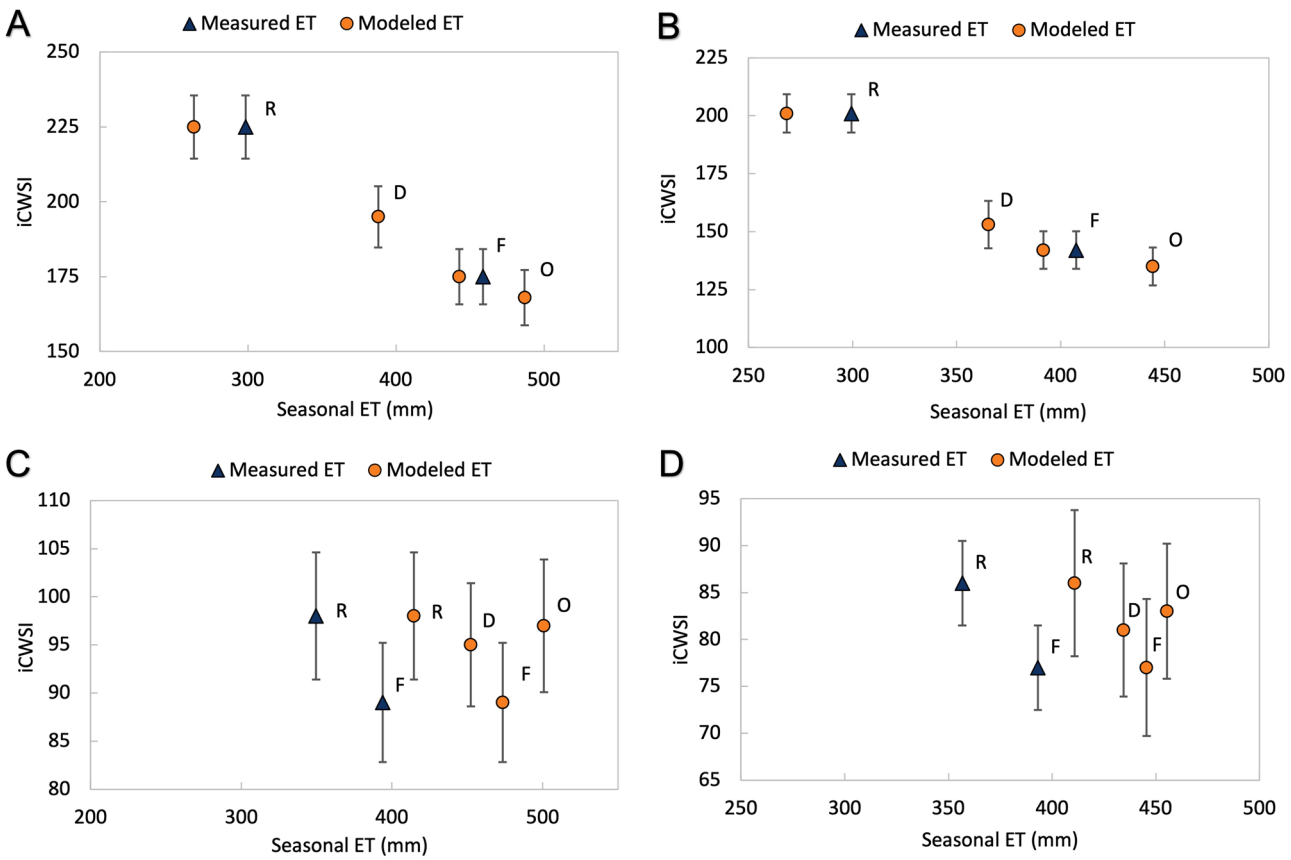

Fig. 7. Mean iCWSI vs. seasonal ET for 2020 and 2021: A) maize 2020, B) soybean 2020, C) maize 2021, and D) soybean 2021. The labels used for data points include 'R' for rainfed, 'D' for deficit, 'F' for full, and 'O' for over. The error bars on each data point denotes the standard error in computation of mean iCWSI for each level.

between data points for each level for 2020 as compared with data from 2021. The data points for each level had more overlap in 2021. This overlap in data was caused by the variability in prescribed irrigation within a level. The range of prescribed irrigation for the full irrigation plots was about 39 mm in 2020 and about 73 mm in 2021. Although the range of irrigation in the full irrigated plots was larger in 2021, mean irrigation applied in 2020 was substantially larger than in 2021 (Table 1). In summary, a significant positive increase in crop yield with crop ET was found for the rainfed and deficit levels for both crops in 2020. Further, the mean seasonal modeled ET increased from rainfed to full by 59 mm in maize and 29 mm in soybean in 2021. This increase in ET on average from rainfed to full using the measured data (neutron probe data with seasonal water balance) was 44 mm in maize and 36 mm in soybean in 2021. While a considerable increase in crop ET was observed from rainfed to full, there were no significant differences in yield found in 2021 between the irrigation levels. This also demonstrated that the reduction in ET for rainfed did not result in loss of carbon assimilation and hence, similar crop yield among the rainfed and irrigated methods.

It is evident from the data presented in the previous sections that larger seasonal crop ET did not result in improved crop yield for all cases. Additionally, the crop water stress was detected using IRTs in cases where there were no yield losses and considerable reductions in crop ET as compared to the full irrigation level. This observation was true for rainfed and deficit irrigation levels in 2021 since there were no yield differences among the levels. The seasonal iCWSI, ET, and crop yield data from soybean in 2020 were used to demonstrate the different stages of crop water stress (Table 6). It can be observed from the table that the mean iCWSI is increasing with higher crop water stress, mean ET is reducing with higher crop water stress, and crop yield is similar between the well-watered and low crop water stress cases. Hence, the data from the study supports the hypothesis that the IRTs can be used to detect crop water stress by sensing increased canopy temperature before the onset of yield limiting or carbon-dioxide-limiting water stress.

The study highlighted that the reduction in stomatal conductance and evapotranspiration does not result in loss of carbon assimilation and crop yield instantaneously. This inference is crucial for using thermal sensors (IRTs) for full irrigation management to achieve maximum crop yield. Thermal sensors rely on sensing increased canopy temperature as a signal for crop water stress. This study presented the case that the increased canopy temperature due to partial stomatal closure does not result in yield loss during the early phase. Hence, the thermal sensors can be effective for irrigation management in the well-watered crop. Previous research studies have confirmed that the rate of stomatal conductance is reduced at a faster rate as compared with reduction in the carbon assimilation under water deficit conditions (Chaves and Oliveira, 2004). Water consumption by plants can be reduced by manipulating stomatal functioning without affecting plant functioning and growth (Loveys and Davies, 2004). On the contrary, many studies assume instantaneous yield reduction with the development of crop water stress (Holzman et al., 2018; Peters and Evett, 2008; Zhang et al., 2021b). Future studies should investigate whether the concept of energy-limiting water stress is observed in other climates and provide recommendations on management of irrigation using thermal sensing.

This research presented data from two growing seasons and computed iCWSI thresholds for the sub-humid climate of Eastern Nebraska. Therefore, these results are representative of the corn-soybean producing fields in sub-humid portion of the Central Great Plains. Since the crop water stress in 2021 was observed to be mild on most days, data from only the 2020 growing season was used in

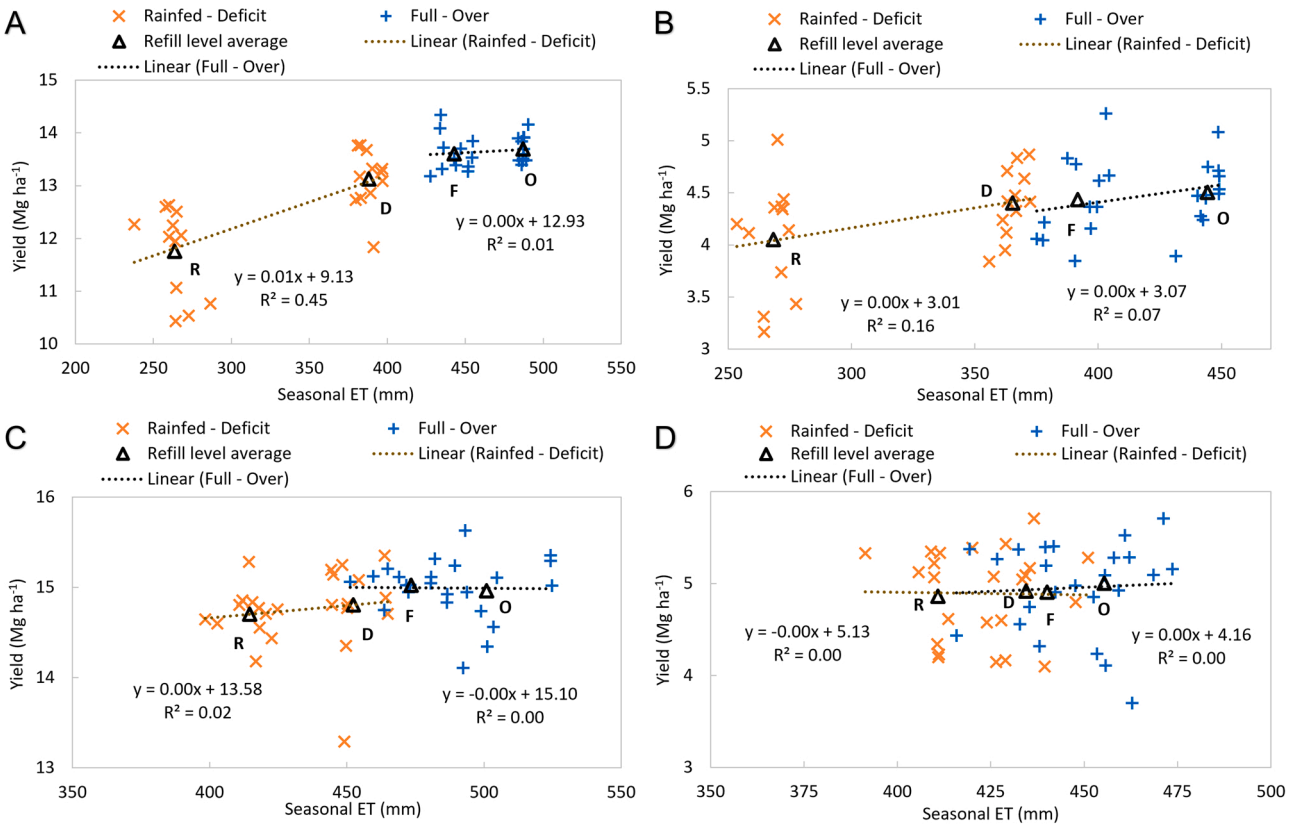

Fig. 8. Seasonal crop evapotranspiration vs. crop yield for A) maize 2020, B) soybean 2020, C) maize 2021, and D) soybean 2021. The labels used for averaged data points include 'R' for rainfed, 'D' for deficit, 'F' for full, and 'O' for over.

Table 6
Integrated crop water stress index (iCWSI), evapotranspiration, and crop yield from soybean in 2020 demonstrating the three conditions of water stress. The data from rainfed, deficit, and full irrigation levels are used to represent no water stress, low water stress, and high water stress, respectively.

Condition	iCWSI	Evapotranspiration (mm)	Yield (Mg ha^{-1})
No water stress (Energy-limiting photosynthesis)	140	417	4.4
Low water stress (Energy-limiting photosynthesis)	153	365	4.4
High water stress (Carbon-dioxide-limiting photosynthesis)	201	310	4.0

computing the iCWSI irrigation thresholds. The thresholds computed do not include year-to-year variability in weather and crop water stress. Hence, data from at least two additional seasons should be incorporated to strengthen the representativeness of these thresholds. Further, these thresholds may not be applicable in other geographic locations, particularly in drier climates. The absence of a zone control variable rate irrigation system restricted the randomization of different irrigation refill level plots across the field. This study utilized a speed control system since this system was more commonly used by producers and was lower cost than a zone control system. Future research can include a zone control system to distribute treatments with more flexibility across the field and improve the randomization of treatments. Additional research is warranted to investigate the transition from the energy-limiting water stress to the carbon dioxide-limiting water stress and the factors affecting the timing of this transition. This study draws conclusions about stomatal conductance from the measured evapotranspiration data. Future studies could incorporate direct measurement of stomatal conductance when studying effects of varying levels of water stress on evapotranspiration, yield, and carbon assimilation.

4. Conclusions

This two-year study evaluated the use of pivot-mounted IRTs for the detection of crop water stress in maize and soybean. This research was successful in detecting crop water stress from thermal sensors in fully irrigated plots without incurring crop yield loss (i.e., detecting energy-limiting water stress before carbon-dioxide-limiting water stress occurs). Contrary to the common assumption, a reduction in seasonal crop ET did not always result in lower crop yield. Mild crop water stress for a short period of time may not lead to crop yield loss. This finding is fundamental for management of full irrigation using thermal sensing to achieve potential yield. Significant ET-yield correlations were observed only with rainfed and deficit levels in 2020. The mean iCWSI and seasonal ET for each level was found to be negatively related for both 2020 and 2021. It was found that the iCWSI substantially increased after two days from a wetting event.

The low, medium, and high iCWSI thresholds for irrigation management were determined as 120, 150, and 180, respectively for maize and 110, 130, and 150, respectively for soybean. These thresholds are applicable for the sub-humid climate of the Central Great Plains. It is proposed that two more seasons of iCWSI data from this region should be incorporated into the developed thresholds to account for variability among the seasons. Future research should implement the developed iCWSI thresholds for management of irrigation and validate their use for the sub-humid climate.

Declaration of Competing Interest

The authors declare the following financial interests/personal relationships which may be considered as potential competing interests: Derek Heeren reports financial support and equipment or supplies were provided by Valmont Industries, Inc. Steve Evett has patent #8924,031 B1, Irrigation scheduling and supervisory control and data acquisition system for moving and static irrigation systems. Susan O'Shaughnessy has patent #8924,031 B1, Irrigation scheduling and supervisory control and data acquisition system for moving and static irrigation systems. Steve Evett has patent #8947102 B1, Soil water and conductivity sensing system, joint with Acclima, Inc. Susan O'Shaughnessy has patent #9866,768 B1, Computer vision qualified infrared temperature sensor. Steve Evett has patent #9866,768 B1, Computer vision qualified infrared temperature sensor.

Data availability

Data will be made available on request.

Acknowledgements

The funding for this research was provided by the Irrigation Innovation Consortium, Valmont Industries, and the Robert B. Daugherty Water for Food Global Institute at the University of Nebraska. The authors thank Mr. Mark Schroeder and his team from the University of Nebraska's Eastern Nebraska Research and Extension Center for their cooperation and help with field operations. We also acknowledge personnel from the Biological Systems Engineering Department at the University of Nebraska-Lincoln for their support and help throughout the experiment. The weather data was accessed from the Automated Weather Data Network of the High Plains Regional Climate Center. We are thankful to Mr. Pradhyun Kashyap for his valuable review of the manuscript.

References

Aladenola, O., Madramootoo, C., 2014. Response of greenhouse-grown bell pepper (Capsicum annuum L.) to variable irrigation. Can. J. Plant Sci. 94, 303–310. https://doi.org/10.4141/CJPS2013-048.

Allen, R.G., Pereira, L.S., Raes, D., Smith, M., 1998. Crop evapotranspiration: Guidelines for computing crop water requirements, Irrigation and Drainage Paper 56, Rome, Italy: Food and Agriculture Organization of the United Nations.

Barker, J.B., Heeren, D.M., Neale, C.M.U., Rudnick, D.R., 2018. Evaluation of variable rate irrigation using a remote-sensing-based model. Agric. Water Manag. 203, 63–74. https://doi.org/10.1016/j.agwat.2018.02.022.

Berni, J.A.J., Zarco-Tejada, P.J., Sepulcre-Cantó, G., Fereres, E., Villalobos, F., 2009. Mapping canopy conductance and CWSI in olive orchards using high resolution thermal remote sensing imagery. Remote Sens. Environ. 113, 2380–2388. https://doi.org/10.1016/j.rse.2009.06.018.

Bhatti, S., Heeren, D.M., Barker, J.B., Neale, C.M.U., Woldt, W.E., Maguire, M.S., Rudnick, D.R., 2020. Site-specific irrigation management in a sub-humid climate using a spatial evapotranspiration model with satellite and airborne imagery. Agric. Water Manag. 230, 105950 https://doi.org/10.1016/j.agwat.2019.105950.

Bhatti, S., Heeren, D.M., Shaughnessy, S.A.O., Evett, S.R., Maguire, M.S., Kashyap, S.P., Neale, C.M.U., 2022. Comparison of stationary and mobile canopy sensing systems for maize and soybean in Nebraska, USA. Appl. Eng. Agric. 38, 331–342. https://doi.org/10.13031/aea.14945.

Bierhuizen, J.F., Slatyer, R.O., 1965. Effect of atmospheric concentration of water vapour and CO_2 in determining transpiration-photosynthesis relationships of cotton leaves. Agric. Meteorol. 2, 259–270. https://doi.org/10.1016/0002-1571(65)90012-9.

Campos, I., Neale, C.M.U., Suyker, A.E., Arkebauer, T.J., Gonçalves, I.Z., 2017. Reflectance-based crop coefficients REDUX: For operational evapotranspiration estimates in the age of high producing hybrid varieties. Agric. Water Manag 187, 140–153. https://doi.org/10.1016/j.agwat.2017.03.022.

Chaves, M.M., Oliveira, M.M., 2004. Mechanisms underlying plant resilience to water deficits: prospects for water-saving agriculture. J. Exp. Bot. 55, 2365–2384. https://doi.org/10.1093/jxb/erh269.

DeJonge, K.C., Taghvaeian, S., Trout, T.J., Comas, L.H., 2015. Comparison of canopy temperature-based water stress indices for maize. Agric. Water Manag 156, 51–62. https://doi.org/10.1016/j.agwat.2015.03.023.

Djaman, K., Irmak, S., 2012. Soil water extraction patterns and crop, irrigation, and evapotranspiration water use efficiency of maize under full and limited irrigation and rainfed settings. Trans. Asabe 55, 1223–1238.

Durand, M., Murchie, E.H., Lindfors, A.V., Urban, O., Aphalo, P.J., Robson, T.M., 2021. Diffuse solar radiation and canopy photosynthesis in a changing environment. Agric. . Meteorol. 311. https://doi.org/10.1016/j.agrformet.2021.108684.

Eck, H.V., 1986. Effects of water deficits on yield, yield components, and water use efficiency of irrigated corn1. Agron. J. 78, 1035–1040. https://doi.org/10.2134/agronj1986.00021962007800060020x.

Evett, S.R., O'Shaughnessy, S.A., Peters, R.T., 2014. Irrigation scheduling and supervisory control and data acquisition system for moving and static irrigation systems. US Pat. 8 (924), 031.

Evett, S.R., Shaughnessy, S.A.O., Andrade, M.A., Colaizzi, P.D., 2020. Theory and development of a vri decision support system: the usda-ars isscada approach. Trans. Asabe 63, 1507–1519.

Fereres, E., Soriano, M.A., 2007. Deficit irrigation for reducing agricultural water use. J. Exp. Bot. 58, 147–159. https://doi.org/10.1093/jxb/erl165.

Garrity, D.P., Watts, D.G., Sullivan, C.Y., Gilley, J.R., 1982. Moisture deficits and grain sorghum performance: evapotranspiration-yield relationships1. Agron. J. 74, 815–820. https://doi.org/10.2134/agronj1982.00021962007400050011x.

Han, M., Zhang, H., DeJonge, K.C., Comas, L.H., Trout, T.J., 2016. Estimating maize water stress by standard deviation of canopy temperature in thermal imagery. Agric. Water Manag 177, 400–409. https://doi.org/10.1016/j.agwat.2016.08.031.

Hanks, R.J., 1974. Model for predicting plant yield as influenced by water use. Agron. J. 66, 660–665. https://doi.org/10.2134/agronj1974.00021962006600050017x.

Holzman, M.E., Carmona, F., Rivas, R., Niclòs, R., 2018. Early assessment of crop yield from remotely sensed water stress and solar radiation data. ISPRS J. Photogramm. Remote Sens 145, 297–308. https://doi.org/10.1016/j.isprsjprs.2018.03.014.

Huete, A.R., 1988. A soil-adjusted vegetation index (SAVI. Remote Sens. Environ. 25, 295–309. https://doi.org/10.1016/0034-4257(88)90106-X.

Irmak, S., 2015. Interannual variation in long-term center pivot–irrigated maize evapotranspiration and various water productivity response indices. I: grain yield, actual and basal evapotranspiration, irrigation-yield production functions, evapotranspiration-yield produc. J. Irrig. Drain. Eng. 141, 04014068. https://doi.org/10.1061/(asce)ir.1943-4774.0000825.

Jackson, R.D., Idso, S.B., Reginato, R.J., Pinter Jr., P.J., 1981. Canopy temperature as a crop water stress indicator. Water Resour. Res. 17, 1133–1138. https://doi.org/10.1029/WR017i004p01133.

Kashyap, S.P., 2021. High-Frequency Unmanned Aircraft Flights For Crop Canopy Imaging During Diurnal Moisture Stress. University of Nebraska-Lincoln.

Ko, J., Piccinni, G., 2009. Corn yield responses under crop evapotranspiration-based irrigation management. Agric. Water Manag 96, 799–808. https://doi.org/10.1016/j.agwat.2008.10.010.

Kullberg, E.G., DeJonge, K.C., Chávez, J.L., 2017. Evaluation of thermal remote sensing indices to estimate crop evapotranspiration coefficients. Agric. Water Manag 179, 64–73. https://doi.org/10.1016/j.agwat.2016.07.007.

Lena, B.P., Ortiz, B.V., Jiménez-López, A.F., Sanz-Sáez, Á., O'Shaughnessy, S.A., Durstock, M.K., Pate, G., 2020. Evaluation of infrared canopy temperature data in relation to soil water-based irrigation scheduling in a humid subtropical climate. Trans. Asabe 65, 1217–1231. https://doi.org/10.13031/TRANS.13912.

Lobell, D.B., Hammer, G.L., Chenu, K., Zheng, B., Mclean, G., Chapman, S.C., 2015. The shifting influence of drought and heat stress for crops in northeast Australia. Glob. Chang. Biol. 21, 4115–4127. https://doi.org/10.1111/gcb.13022.

Loveys, B.R., Davies, W.J., 2004. Physiological approaches to enhance water use efficiency in agriculture: exploiting plant signalling in novel irrigation practice. In: Bacon, M.A. (Ed.), Water Use Efficiency in Plant Biology. Blackwell Publishing, Oxford, pp. 113–141.

Masseroni, D., Ortuani, B., Corti, M., Gallina, P.M., Cocetta, G., Ferrante, A., Facchi, A., 2017. Assessing the reliability of thermal and optical imaging techniques for detecting crop water status under different nitrogen levels. Sustain 9, 1–20. https://doi.org/10.3390/su9091548.

Medlyn, B.E., Duursma, R.A., Eamus, D., Ellsworth, D.S., Prentice, I.C., Barton, C.V.M., Crous, K.Y., De Angelis, P., Freeman, M., Wingate, L., 2011. Reconciling the optimal and empirical approaches to modelling stomatal conductance. Glob. Chang. Biol. 17, 2134–2144. https://doi.org/10.1111/j.1365-2486.2010.02375.x.

Moran, M.S., Clarke, T.R., Inoue, Y., Vidal, A., 1994. Estimating crop water deficit using the relation between surface-air temperature and spectral vegetation index. Remote Sens. Environ. 49, 246–263. https://doi.org/10.1016/0034-4257(94)90020-5.

Musick, J.T., Dusek, D.A., 1978. Irrigated corn yield response to water. Pap. - Am. Soc. Agric. Eng. https://doi.org/10.13031/2013.34531.

Neale, C.M.U., Geli, H.M.E., Kustas, W.P., Alfieri, J.G., Gowda, P.H., Evett, S.R., Prueger, J.H., Hipps, L.E., Dulaney, W.P., Chávez, J.L., French, A.N., Howell, T.A., 2012. Soil water content estimation using a remote sensing based hybrid evapotranspiration modeling approach. Adv. Water Resour. 50, 152–161. https://doi.org/10.1016/j.advwatres.2012.10.008.

O'Shaughnessy, S.A., Evett, S.R., Colaizzi, P.D., Howell, T.A., 2013. Wireless sensor network effectively controls center pivot irrigation of sorghum. Appl. Eng. Agric. 29, 853–864. https://doi.org/10.13031/aea.29.9921.

O'Shaughnessy, S.A., Andrade, M.A., Evett, S.R., 2017. Using an integrated crop water stress index for irrigation scheduling of two corn hybrids in a semi-arid region. Irrig. Sci. 35, 451–467. https://doi.org/10.1007/s00271-017-0552-x.

O'Shaughnessy, S.A., Kim, M., Andrade, M.A., Colaizzi, P.D., Evett, S.R., 2020. Site-specific irrigation of grain sorghum using plant and soil water sensing feedback - Texas High Plains. Agric. Water Manag 240, 106273. https://doi.org/10.1016/j.agwat.2020.106273.

Osroosh, Y., Peters, R.T., Campbell, C.S., Zhang, Q., 2016. Comparison of irrigation automation algorithms for drip-irrigated apple trees. Comput. Electron. Agric. 128, 87–99. https://doi.org/10.1016/j.compag.2016.08.013.

Payero, J.O., Irmak, S., 2006. Variable upper and lower crop water stress index baselines for corn and soybean. Irrig. Sci. 25, 21–32. https://doi.org/10.1007/s00271-006-0031-2.

Payero, J.O., Melvin, S.R., Irmak, S., Tarkalson, D., 2006. Yield response of corn to deficit irrigation in a semiarid climate. Agric. Water Manag 84, 101–112. https://doi.org/10.1016/j.agwat.2006.01.009.

Peters, R.T., Evett, S.R., 2004. Modeling diurnal canopy temperature dynamics using one-time-of-day measurements and a reference temperature curve. Agron. J. 96, 1553–1561. https://doi.org/10.2134/agronj2004.1553.

Peters, R.T., Evett, S.R., 2008. Complete center pivot automation using the temperature-time threshold method of irrigation scheduling. J. Irrig. Drain. Eng. 134, 286–291. https://doi.org/10.13031/2013.16409.

Pezeshki, S.R., 2001. Wetland plant responses to soil flooding. Environ. Exp. Bot. 46, 299–312. https://doi.org/10.1007/978-3-319-13368-3_5.

Rossini, M., Fava, F., Cogliati, S., Meroni, M., Marchesi, A., Panigada, C., Giardino, C., Busetto, L., Migliavacca, M., Amaducci, S., Colombo, R., 2013. Assessing canopy PRI from airborne imagery to map water stress in maize. ISPRS J. Photogramm. Remote Sens. 86, 168–177. https://doi.org/10.1016/j.isprsjprs.2013.10.002.

Schneekloth, J.P., Klocke, N.L., Hergert, G.W., Martin, D.L., Clark, R.T., 1991. Crop rotations with full and limited irrigation and dryland management. Trans. Am. Soc. Agric. Eng. 34, 2372–2380. https://doi.org/10.13031/2013.31882.

Singh, J., Ge, Y., Heeren, D.M., Walter-Shea, E., Neale, C.M.U., Irmak, S., Woldt, W.E., Bai, G., Bhatti, S., Maguire, M.S., 2021. Inter-relationships between water depletion and temperature differential in row crop canopies in a sub-humid climate. Agric. Water Manag 256, 107061. https://doi.org/10.1016/j.agwat.2021.107061.

Stone, K.C., Bauer, P.J., O'Shaughnessy, S., Andrade-Rodriguez, A., Evett, S., 2020. A variable-rate irrigation decision support system for corn in the U.S. Eastern Coastal plain. Trans. Asabe 65, 1295–1303. https://doi.org/10.13031/TRANS.13965.

Taghvaeian, S., Chávez, J.L., Hansen, N.C., 2012. Infrared thermometry to estimate crop water stress index and water use of irrigated maize in northeastern colorado. Remote Sens 4, 3619–3637. https://doi.org/10.3390/rs4113619.

Upchurch, D.R., Wanjura, D.F., Burke, J.J., Mahan, J.R., 1996. Biologically-identified optimal temperature interactive console (BIOTIC) for managing irrigation. US Pat.

Vories, E., O'Shaughnessy, S., Sudduth, K., Evett, S., Andrade, M., Drummond, S., 2020. Comparison of precision and conventional irrigation management of cotton and impact of soil texture. Precis. Agric. https://doi.org/10.1007/s11119-020-09741-3.

Wanjura, D.F., Upchurch, D.R., Mahan, J.R., 1995. Control of irrigation scheduling using temperature-time thresholds. Trans. Am. Soc. Agric. Eng. 38, 403–409. https://doi.org/10.13031/2013.27846.

Wu, X., Tang, Y., Li, C., McHugh, A.D., Li, Z., Wu, C., 2018. Individual and combined effects of soil waterlogging and compaction on physiological characteristics of wheat in southwestern China. F. Crop. Res 215, 163–172. https://doi.org/10.1016/j.fcr.2017.10.016.

Zhang, H., Xiong, Y., Huang, G., Xu, X., Huang, Q., 2017. Effects of water stress on processing tomatoes yield, quality and water use efficiency with plastic mulched drip irrigation in sandy soil of the Hetao Irrigation District. Agric. Water Manag 179, 205–214. https://doi.org/10.1016/j.agwat.2016.07.022.

Zhang, J., Guan, K., Peng, B., Jiang, C., Zhou, W., Yang, Y., Pan, M., Franz, T.E., Heeren, D.M., Rudnick, D.R., Abimbola, O., Kimm, H., Caylor, K., Good, S., Khanna, M., Gates, J., Cai, Y., 2021a. Challenges and opportunities in precision irrigation decision-support systems for center pivots. Environ. Res. Lett. 16. https://doi.org/10.1088/1748-9326/abe436.

Zhang, J., Guan, K., Peng, B., Pan, M., Zhou, W., Jiang, C., Kimm, H., Franz, T.E., Grant, R.F., Yang, Y., Rudnick, D.R., Heeren, D.M., Suyker, A.E., Bauerle, W.L., Miner, G.L., 2021b. Sustainable irrigation based on co-regulation of soil water supply and atmospheric evaporative demand. Nat. Commun. 12, 1–10. https://doi.org/10.1038/s41467-021-25254-7.